A SAILPLANE WING CONSTRUCTED OF FOAM CORE AND POLYESTER FIBERGLASS SKIN

By

Ronald D Kriz

California Polytechnic State University

San Luis Obispo

1973

Submitted:_____

Grade:_____

Project Advisor:_____

Department Head
Approval:_____

TABLE OF CONTENTS

LIST OF FIGURES

LIST OF TABLES

SUMMARY

The results from a stress analysis of a thin skin, foam core, high aspect ratio wing indicate a possible method of constructing sailplane wings. The analysis includes an approximation of the maximum core and skin shear stress, a computer program to evaluate the stress distribution and displacements of a thin walled unsymmetrical tapered cylinder, and the accountability of creep.

THEORY OF COMPOSITE BEAMS

Composite beams are designed so that each material in the beam is most efficiently used with respect to weight, position, and resistance to forces.

Take for example the beam shown in Figure 2. The flange material is positioned so that it resists the maximum normal and shear stresses. Therefore a high modulus material should be used. The core material is positioned so that it spaces the flange material and resists the maximum shear stress. A lighter weight material is choosen for the core material because it occupies the most volume of the beam. But the lighter weight core materials usually have lower alowable maximum normal and shear stresses. This is of no consequence because the core's normal stress is small ($E_{core} << E_{skin}$) and the core's maximum allowable shear stress is within working limits. So the only two limitations are the flange's maximum allowable normal stress and the core's maximum allowable shear stress. With these two design requirements a beam can be designed with a tolerable reduction in maximum strength and a substantial savings in weight.

The construction of most high aspect ratio sailplane wings today include one spar, ribs, and a thin skin, Figure 3A. Most of the high performance europian sailplanes have wings constructed of spar and thick skin with no ribs, Figure 3B. The skin has a composite sandwich construction with a foam core laminated between layers of resin and glass cloth. The spar is usually constructed from epoxy resins and glass fabric. In such a construction the

skin resists most of the normal forces and the shear webs in the spar resists some of the shear forces. The shear webs are kept thin as in an I-beam to make efficient use of weight. The idea of using a different type of shear web such as foam core is possible so long as the same shear stress requirements is sateisfied. Buckling of the skin is at present resisted by the thick laminated skin. The thick box beam spar also resists buckling of the thick skin because of the short chord. The use of a foam core would also resist buckling. Therefore the use of a low density foam core instead of a thin higher density shear web is completely with in reason. And such is the objective of this senior project, to structually evaluate a high aspect ratio wing constructed of foam core and resin-glass skin.

SYMBOLS

E_c	Modulus Of Elasitcity For The Core
b	Width Of The Composite Beam Crossection
d	Total Thickness Of Composite Beam
μ	Poisson's Ratio
τ_{max}	Maximum Shear Stress
$\tau_{c_{max}}$	Maximum Core Shear Stress
$\tau_{s_{max}}$	Maximum Skin Shear Stress
t_{shear}	Skin Thickness That Resists $\tau_{s\ max}$
$\sigma_{s\ ultimate}$	Skin Ultimate Normal Stress
t_{Normal}	Skin Thickness That Resists $\sigma_{s\ ultimate}$
σ_w	Wrinkling Stress
B_1	Constant
ρ	Constant
t_s	Skin Thickness For Favorable Wing Deflections
t_w	Skin Thickness That Resists σ_w
t	Skin Thickness
E_s	Modulus Of Elasiticity For The Skin
M	Bending Moment
t_c	Core Thickness
w_c	Core Width

SYSTEM DEFINED

The wing crossection was defined as a NACA 4412. The root and tip chord are 8.5 and 4.25 inches respectively with no sweep back at the leading edge, Figure 1. The span was 51.1875 inches with a 17.7 aspect ratio. This particular wing had the same dimensions as a wooden wing used on one of the authors radio-controlled sailplanes. The small size made it practical to build and hopefully at some future time fly.

SKIN-CORE APPROXIMATIONS

As shown in Appendix A the flexural rigidity (bending modulus) of a composite beam shown in Figure 2 is:[2]

$$(EI)_{composite} = \frac{E_s b}{12(1-\mu^2)}\left[d^3 - t_c^3\left(1 - E_c/E_s\right)\right] \qquad (1)$$

For beams in bending the deflection equation shows that the

$$\frac{d^2z}{dy^2} = \frac{M}{(EI)_{composite}} \qquad (2)$$

deflections will depend on the combined rigidity of the skin and core materials.

If $E_c \ll E_s$ then the flexural rigidity is seen to depend only on the skin modulus of elasticity.

$$(EI)_{composite} \simeq \frac{E_s b}{12(1-\mu^2)}\left[d^3 - t_c^3\right] \qquad (3)$$

The percent of deflection due to shear was assumed to be small and therefore neglected, Appendix C.

Unfortunately the core cannot be totally ignored. Although the core does not resist bending it does resist a part of the maximum shear stress and resists buckling of the thin skin.

MAXIMUM SHEAR STRESS

If the airfoil shape is simplified as a rectangular composite beam the formulas used to calculate shear stresses can be used, Appendix D. The equation for the maximum shear stress of a thin skin foam core was derived.

$$\tau_{max} = \tau_{c_{max}} + \tau_{s_{max}} = \frac{V_{max}\left[\frac{2(t_c+d)bt + t_c^2(2t+w_c E_c/E_s)}{8bt+4(2t+w_c E_c/E_s)}\right]\left[bt+(2t+w_c\frac{E_c}{E_s})\frac{t_c}{2}\right]}{\left[b(d^3-t_c^3)+t_c^3(2t+w_c E_c/E_s)\right]\left[2t+w_c E_c/E_s\right]/12} \qquad (4)$$

Using the method of equivalent areas a relation for the shear forces in the core and skin was formulated, Appendix D,

$$\tau_{s_{max}} : \tau_{c_{max}} = 53 \qquad (5)$$

for the airfoil shape at midspan.

By approximating the dimensions of the airfoil at midspan as a rectangular composite beam the equations (4) and (5) were solved simultaneously for core and shear stresses at a maximum shear load of 10 lbs. (7G's).

$$\tau_{c_{max}} = 3.33\ ^{lb}/_{in^2} \qquad \tau_{s_{max}} = 177\ ^{lb}/_{in^2}$$

Skin thickness necessary to resist τ_{max}, Appendix D.

$$t_{shear} = 0.025 \text{ in.}$$

MAXIMUM NORMAL STRESS

An approximate maximum noraml stress at a 7G wing loading is calculated by using the elastic flexural formula. The root airfoil

$$\sigma_{s_{ultimate}} = 6240 \text{ psi} \qquad t_{Normal} = 0.0091 \text{ in.}$$

is approximated as a rectangular crossection so that the moment of inertia can be found as a function fo skin thickness, Appendix E.

SKIN WRINKLING

A method for determining skin thickness required to prevent wrinkling of skin as a function of core and skin properties was outlined by Knight.[1]

The compressive stress in the facing material at which wrinkling will occur is given by:

$$\sigma_w = B_1 E_s^{1/3} E_c^{2/3} \qquad (6)$$

The constant B_1 is plotted as a function of ρ where ρ is given by:

$$\rho = \frac{t_s}{t_c} \left(E_s / E_c \right)^{1/3} \qquad (7)$$

For values of $\rho \leq 0.25$, B_1 is a constant, $B_1 = 0.575$.

$$\sigma_w = 0.575 E_s^{1/3} E_c^{2/3} \qquad (8)$$

Substituting the skin and core modulus of elasticity into (8) gives a wrinkling stress.

$$\sigma_w = 5475 \text{ psi}$$

Considering this as a maximum normal stress. The skin thickness can again be determined as in Appendix E.

$$t_w = 0.011 \text{ m.}$$

THIN WALLED-UNSYMMETRICAL CROSSECTION-TAPERED CYLINDER

The fact that the core properties could be ignored in the composite beams deflections motivated the stress analysis of a thin walled-unsymmetrical crossection-tapered cylinder.

A computer program was written to take any defined shaped thin walled cylinder (wing shape) and give deflections and twists along the span for any defined wing loading, Appendix F.

The program was tested for accuracy by defining a cylinderical shape whose deflections, moments of inertia, shear center location, weight, etc. were compared with hand calculations. The program was found to be very accurate for the thin skin approximation.

APPROXIMATE DEFLECTIONS

The wing was approximated as a rectangular box with a uniform distributed load simulating different G loads, Appendix G. Skin thicknesses sufficient for resisting $\sigma_{s_{ultimate}}$ and buckling produced intolerably large deflections. Therefore the skin thickness was increased so that deflections reasonable for aero-elastic effects would be realized. A final skin thickness was calculated to give reasonable deflections for a 7G simulated load and resist the

$$t_s = 0.025 \text{ in}$$

maximum shear stress.

WING FABRICATION

With regard to money and time the wing was not constructed with the best material or fabrication procedures. Instead relatively inexpensive materials and simplified fabrication methods were used to construct a testable wing. The skin thickness was not closely controlled so long as the thickness was known and related deflections measurable.

The foam core was constructed of CPR 9005-2 rigid urethane foam. Originally it was hoped that the foam core shape could be cut by a hot wire guided over root and tip airfoil templates. Unfortunately it was found difficult to cut urethane foam sections longer then a few feet. The urethane core was therefore shaped by sanding spanwise with the root and tip airfoil templates as guides.

The skin was fabricated by wet lay up of 6 ounce glass cloth and polyester resin. The surface was sanded once and a finish coat applied.

A one inch wide hard wood root airfoil shape was glued to the foam and was also covered by resin and glass. This served as a noncrushable rigid support for the fixed condition of a cantilever beam, Figure 4C, 4B.

TEST PROCEDURE

The wing was mounted in a fixed condition at the root, Figure 4, with the flat side of the airfoil facing upward. The flat side of the wing was leveled so that an evenly distributed load could be applied on the flat surface in a predictable manner. Time and presence of creep permitted only a 1G and 2G load for measuring deflections, Table I.

Wing G loading was simulated by a uniform distributed load using a string of metal slugs attached to a line of tape. The slugs were measured and distributed to simulated a 1G and 2G load. The load was applied to a line drawn from the root aerodynamic center to the tip aerodynamic center.

The wings airfoil shape at the root and tip were measured, Table II. The skin thickness along the span was measured, Table III. A piece of the skin was removed from the wing and tensile tested for a modulus of elasticity, Table V. The above was substituted into the computer program to obtain the calculated deflections which are compared with the experimental deflections in Table I.

RESULTS AND DISCUSSION

The deflections were calculated assuming the core was insignifcant in resisting bending. The modulus of the core and skin were experimentally measured and the term

$$\left(1 - E_c/E_s\right) \qquad (9)$$

in the composite flexural rigidity equation was found to be so nearly equal to one that the core had little or no effect on the composite beams deflections, Appendix B. The experimental deflections varified that this was a good approximation, Table I. The percent error in deflections are a combination of, the core materials contribution to resisting bending, accuracy of deflection measurements, creep, and numerical methods used to calculate deflections. The core's contribution in resisting deflection, although shown to be small, account for the smallest of the possible error sources. Creep is the largest contributor, since the percent errors are seen to be higher for the larger G loads. The error in measuring the deflections with a 1 inch travel 0.001 inch dial gage was less then 1%. The error in the numerical methods is shown to be less then 1%, Appendix F.

The presence of creep was noted, Table IV. For the wing being tested, little should be said about the creep since the fabrication methods and materials were not the optimum. But creep can and should be accounted for in reinforced plastics who's materials and

fabrication are more closely controlled. A method for determining time, temperature, and rupture stresses in reinforced plastics shows that creep in reinforced plastics can withstand large stresses for long periods of time at room temperatures.[3] For example from a series of tests Plaskon 920 (a polyester resin-glass laminate) can resist a stress of 28,500 psi for more then five years before rupture.[3] It was found that these long stress to rupture estimates could be accurately predicted by a relation derived by Larson and Miller.[3]

$$T(20 + \log t) = \text{constant}$$

T = Temperature
t = Time

So that long-time low temperature creep results could be calculated from data of short-time high temperature creep tests.

The shear stress distribution used to calculate the shear center location for a thin walled unsymmetrical tapered cylinder is questionably used for the composite wing since it has already been shown that the core material resists a substantial portion of the total shear load, Appendix D.

The normal skin stresses calculated by the computer program accurately predicts the real stress experienced by the composite wing since it has already been shown that the skin resist almost all the bending in the beam.

The foam core as was previous shown resist only the maximum core shear stress. Unfortunately the lowest density foam core has an ultimate shear stress much greater than the maximum core shear stress. A lower density foam could be used so that a lighter wing

will result without lowering the ultimate shear stress past the maximum core shear stress. As of now the wing in comparsion with an identical wing made of wood is about twice as heavy.

It can be shown that the modulus of elasticity for glass-fiber-reinforced polyester resins vary a small amount with respect to the orientation of the glass cloth weave.[4]

CONCLUSIONS

The computer program used to calculated deflections and normal stresses for the thin skin only, are the same deflections and skin stresses existing for the composite (skin and foam) so long as the term

$$(1 - E_c/E_s)$$

in the flexural rigidity of a composite is approximately equal to one.

Creep in glass reinforced plastics at room temperatures can withstand large stresses for long periods of time before rupture.

Skin thicknesses adequate to resist the maximum normal stresses and buckling produced inadequately large deflections. The skin thickness depends only on the desired magnitude of deflectinns and the maximum skin shear stress.

The foam core resist only the maximum core shear stress and therefore the lowest density necessary to safely resist this shear stress should be used.

RECOMENDATIONS

It is now possible with the established methodology to optimize such a wing with respect to weight and strength. Time did not permit optimization of the composite wing and the lack of information on the construction of present sailplane wings did not justify a comparision. The author feels that both points should be covered before any large wing fabrication is considered.

At best this senior project demonstrates that such a wing is possible to analize, build, and could possibly be competative with the present high aspect ratio sailplane wings.

As already pointed out the shear center location, although accurately calculated for the thin skin only, was not proven to be accurate for the composite case. Specially shaped composite beams can be constructed so that the emperical shear center location for the composite beam could be compared with the location calculated by the skin approximation method.

REFERENCES

1. Knight, R.S., Analysis Of A Sandwich Construction Glider Wing Design Using Different Foam Plastic Core Materials, Senior Project, California Polytechnic State University Pomona, 1971, pg 37-39.

2. Hexcel, Design Handbook For Honeycomb Sandwich Structures, TSB 123, March 1970, pg 2.8.

3. Goldfein, S., Time-Timperature and Rupture Stresses in Reinforced Plastics, "Modern Plastics", 32(4): 148(dec 1954).

4. McClintock F.A. and Argon A.S., Mechanical behavior of Materials, Addison-Wesley, 1966, pg 87.

5. Bruhn E.F., Analysis And Desin Of Flight Vehicle Structures, Tri-state Offset Company, 1965, pg A15.2-A15.3.

FIGURES AND TABLES

ROOT DIMENSIONS

PNT	X	Z
1	0.000	0.000
2	1.500	0.000
3	2.500	0.000
4	3.500	0.000
5	4.250	0.000
6	5.000	0.000
7	5.500	0.000
8	6.000	0.000
9	6.500	0.000
10	7.250	0.000
11	7.750	0.050
12	8.000	0.070
13	8.250	0.100
14	8.350	0.110
15	8.400	0.140
16	8.450	0.190
17	8.500	0.310
18	8.450	0.450
19	8.400	0.490
20	8.350	0.520
21	8.250	0.570
22	8.000	0.660
23	7.75	0.725
24	7.250	0.825
25	6.500	0.900
26	6.000	0.925
27	5.500	0.925
28	5.000	0.900
29	4.250	0.825
30	3.500	0.725
31	2.500	0.550
32	1.500	0.350

TIP DIMENSION

PNT	X	Z
1	4.250	0.000
2	5.000	0.000
3	5.500	0.000
4	6.000	0.000
5	6.375	0.000
6	6.650	0.000
7	7.000	0.000
8	7.250	0.000
9	7.500	0.000
10	7.875	0.000
11	8.125	0.010
12	8.250	0.020
13	8.375	0.040
14	8.425	0.050
15	8.450	0.060
16	8.475	0.075
17	8.500	0.150
18	8.475	0.225
19	8.450	0.240
20	8.425	0.260
21	8.375	0.280
22	8.250	0.320
23	8.125	0.350
24	7.875	0.409
25	7.500	0.450
26	7.250	0.460
27	7.000	0.460
28	6.750	0.450
29	6.375	0.420
30	6.000	0.375
31	5.500	0.290
32	5.000	0.180

FIGURE 1

WING DIMENSIONS

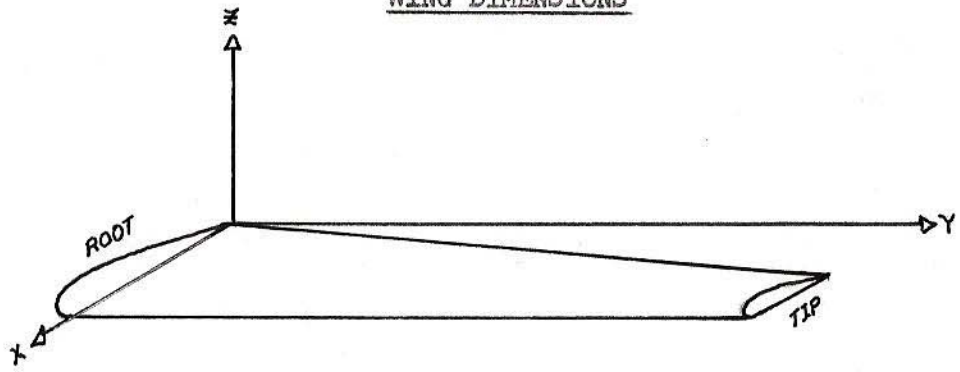

SPAN 51.1875 in.
A.R. 17.7
SKIN THICKNESS 0.030

SCALE 1:1

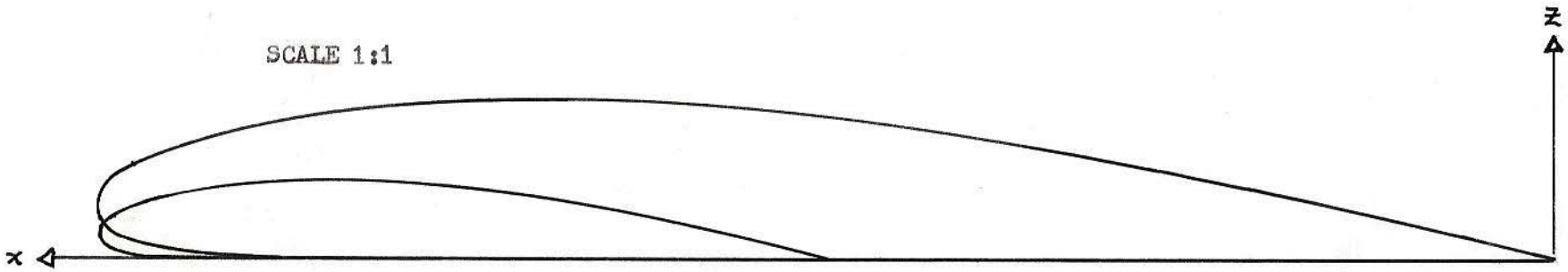

FIGURE 2

COMPOSITE BEAM

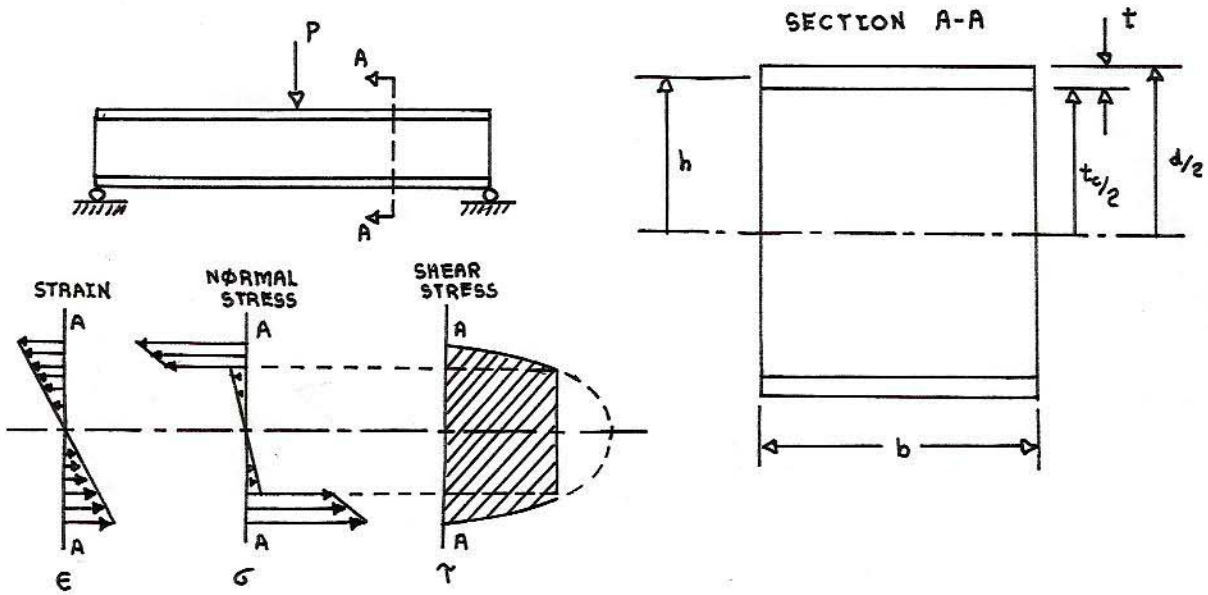

$$\sigma_{max} = \frac{Mh}{I} = \frac{M_{max}}{bt(d-t)}$$

$$\tau_{max} = \frac{VQ}{Ib} = \frac{2V_{max}}{b(t_c+d)}$$

FIGURE 3

WINGS

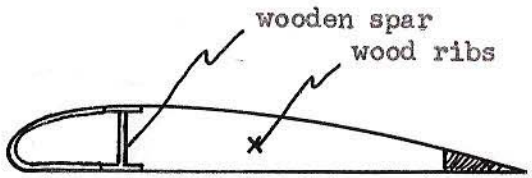

FIGURE 3A

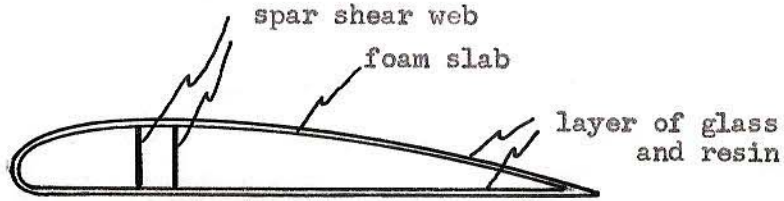

FIGURE 3B

FIGURE 1

TEST SETUP

FIGURE 4A

FIGURE 4B

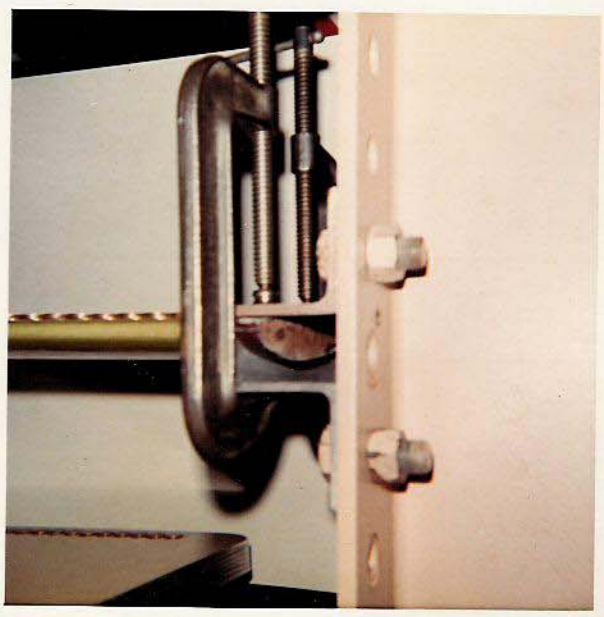

FIGURE 4C

TABLE I

EXPERIMENT DATA

TOTAL WING WEIGHT lb.	CALCULATED	EXPERIMENT	ERROR %
	0.966	0.975	0.93

1G LIFT

UNIFORM LIFT DISTRIBUTION 0.027 lb/in

SPAN LOCATION in inches from ROOT	0	20	30	40	50
EXPERIMENT	0	0.100	0.209	0.333	0.486
CALCULATED	0	0.106	0.224	0.367	0.521
ERROR %	0	5.7	6.7	9.2	6.7

2G LIFT

UNIFORM LIFT DISTRIBUTION 0.054 lb/in

SPAN LOCATION in inches from ROOT	0	20	30	40	50
EXPERIMENT	0	0.200	0.403	0.635	0.931
CALCULATED	0	0.212	0.447	0.734	1.042
ERROR %	0	6.0	11.0	11.9	10.6

Deflections measured by 0.001 inch increment 1 inch travel dial gage.

TABLE II

ROOT-TIP AIRFOIL DIMENSIONS

ROOT AIRFOIL COORDINATES

POINT	X	Z
1	0.000	0.000
2	1.650	0.000
3	2.650	0.000
4	3.650	0.000
5	4.350	0.000
6	5.150	0.000
7	6.150	0.000
8	6.650	0.000
9	7.400	0.000
10	7.875	0.025
11	8.150	0.050
12	8.375	0.100
13	8.475	0.140
14	8.550	0.175
15	8.625	0.225
16	8.660	0.275
17	8.700	0.350
18	8.660	0.450
19	8.625	0.550
20	8.550	0.600
21	8.475	0.650
22	8.375	0.700
23	8.150	0.775
24	7.875	0.850
25	7.400	0.950
26	6.650	1.100
27	6.150	1.025
28	5.150	0.075
29	4.350	0.875
30	3.650	0.800
31	2.650	0.625
32	1.650	0.410

TIP AIRFOIL COORDINATES

POINT	X	Z
1	4.000	0.000
2	5.125	0.000
3	5.625	0.000
4	6.125	0.000
5	6.500	0.000
6	6.875	0.000
7	7.125	0.000
8	7.360	0.000
9	7.625	0.000
10	8.000	0.000
11	8.250	0.000
12	8.400	0.025
13	8.500	0.050
14	8.600	0.075
15	8.650	0.100
16	8.675	0.125
17	8.700	0.175
18	8.675	0.225
19	8.650	0.250
20	8.600	0.300
21	8.500	0.350
21	8.400	0.390
23	8.250	0.425
24	8.000	0.480
25	7.625	0.520
26	7.360	0.525
27	7.125	0.520
28	6.875	0.510
29	6.500	0.490
30	6.125	0.450
31	5.625	0.360
32	5.125	0.260

TABLE III

SKIN THICKNESS AND DENSITY

SPAN LOCATION in inches from ROOT	0	20	30	40	50
SKIN THICKNESS inches	0.031	0.028	0.030	0.032	0.031
DENSITY, lb/in^3	-	0.0351	0.0346	0.0393	-

TABLE IV

CREEP

1G

UNIFORM LIFT DISTRIBUTION
0.027 lb/in

TIME, minutes	0	10	30
TIP DEFLECTIONS inches	0.550	0.615	0.640

RELAXATION

24 HOUR PERIOD TIP DEFLECTION 0.005 in

TABLE V

MATERIAL PROPERTIES

MATERIAL	MODULUS OF ELASTICITY psi	ULTIMATE NORMAL STRESS psi	ULTIMATE SHEAR STRESS psi	DENSITY lb/in^3
CPR 9005-2 URETHANE FOAM	1415	-	20	0.00116
POLYESTER GLASS REINFORCED SKIN	* 6.6×10^5	6240	-	0.0363

* SKIN WAS TENSILE TESTED

SPECIMEN - GAGE LENGTH 6 inches
- WIDTH 1 inch
- GLASS FABRIC ORIENTATION 30 degrees from longitudinal axis

Ultimate Load 190 lbs

Ultimate Stress 6240 psi

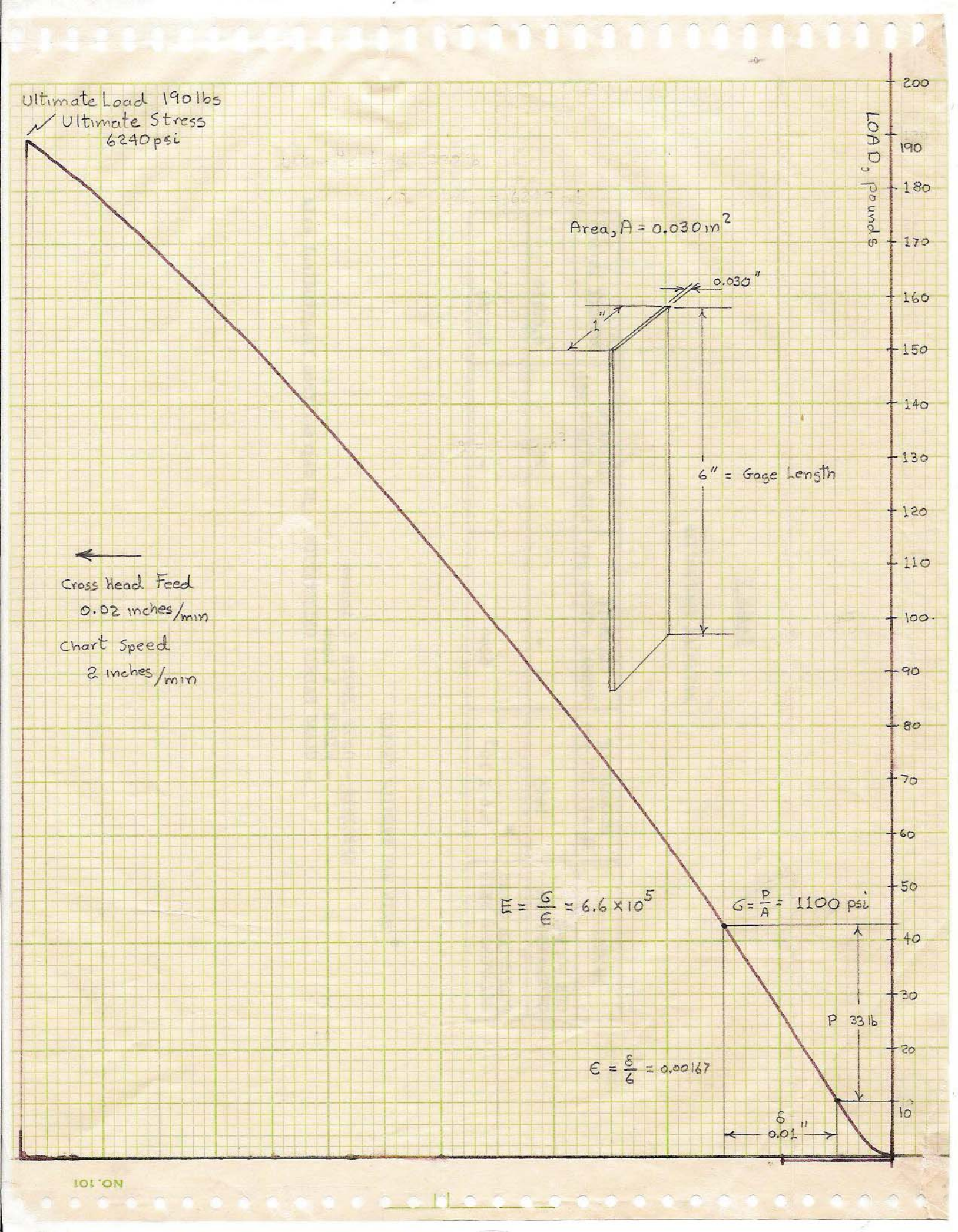

APPENDIX A

FLEXURAL RIGIDITY OF A COMPOSITE BEAM

DERIVATION OF THE FLEXURE RIGIDITY OF A COMPOSITE BEAM

E_c	Modulus of elasticity of the core in the span wise direction
E_s	Modulus of elasticity of the skin
t_c	Thickness of core
d	Total thickness
b	Length of panel edge
	Poisson's ratio of plate
I_s	Moment of inertia of the skin only
D	Flexure rigidity of the composite beam

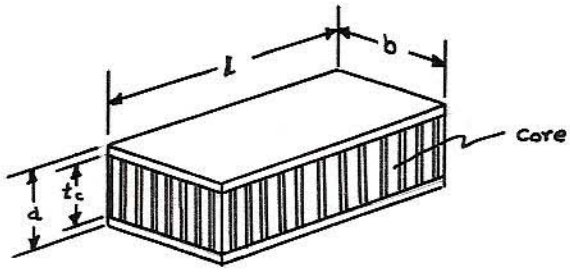

A quick first approximation

$$D \approx E_s I_s = \frac{b E_s}{12} \left[d^3 - t_c^3 \right]$$

A better approximation can be made if we assume that a beam is very wide compared to the depth then the lateral deformation is prevented and the beam is stiffer. In our case we have two face plates whose width $\ggg$ thickness.

Consider a wide beam in pure bending.

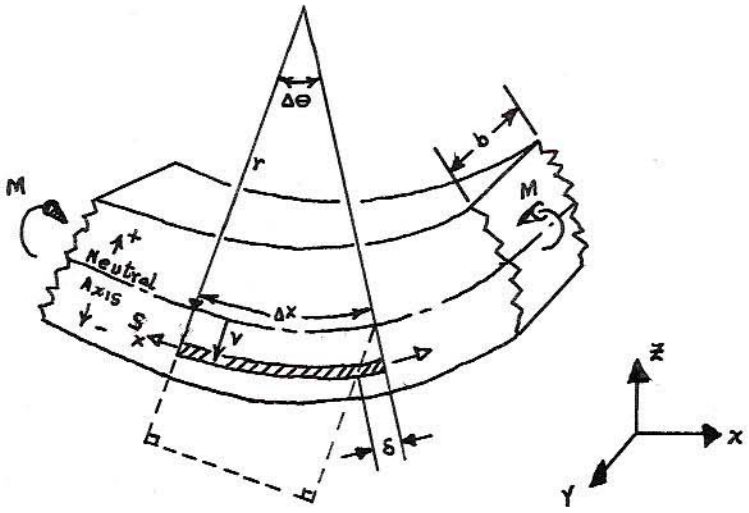

$$\Delta x = r\,\Delta\theta$$

$$\delta = (r+v)\,\Delta\theta - \Delta x$$

$$\delta = v\,\Delta\theta$$

$$\epsilon_x = \frac{\delta}{\Delta x} = \frac{v}{r}$$

Stress occurs on an element of length Δx located a distance v from the neutral axis.

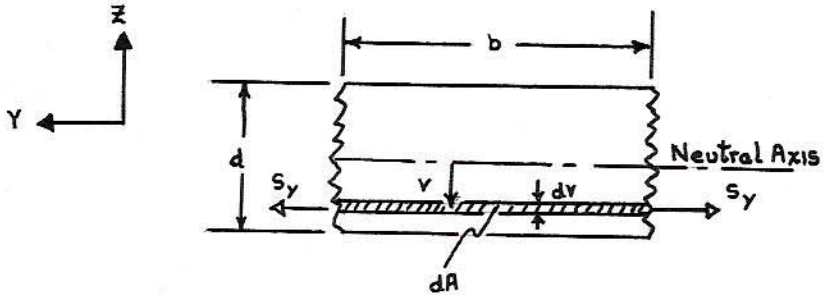

Since lateral movement is prevented therefore $\epsilon_y = 0$

Then S_y is induced in the material to keep sides straight and parallel.

From Hooke's laws assuming $\sigma_z = \tau_{xz} = \tau_{yz} = 0$

$$S_x = \frac{E}{1-\mu^2}\left(\epsilon_x^{\,v/r} + \mu\,\epsilon_y^{\,0}\right) = \frac{Ev}{(1-\mu^2)r}$$

$$M = \int_{area} S_x \, y \, dA \qquad \frac{Eb}{(1-\mu^2)r} \int_{-d/2}^{+d/2} y^2 dV = \frac{Ebd^3}{12(1-\mu^2)r}$$

Recalling the basic relations. $\frac{1}{r} = \frac{M}{EI}$, $D = EI$

$$D = \frac{Ebd^3}{12(1-\mu^2)}$$

For two face plates seperated by core material.

$$D = \frac{E_s b d^3}{12(1-\mu^2)} - \frac{E_s b t_c^3}{12(1-\mu^2)} = \frac{E_s b}{12(1-\mu^2)} \left[d^3 - t_c^3 \right]$$

The idea of adding or subtracting the property of EI for various sections from the original whole crossection can give an even better approximation.

$$D_{core} \simeq \frac{E_c b t_c^3}{12(1-\mu^2)}$$

$$D = \frac{E_s b d^3}{12(1-\mu^2)} - \frac{E_s b t_c^3}{12(1-\mu^2)} + \frac{E_c b t_c^3}{12(1-\mu^2)}$$

$$D = \frac{E_s b}{12(1-\mu^2)} \left[d^3 - t_c^3 \left(1 - E_c/E_s\right) \right]$$

APPENDIX B

CORE MODULUS

CORE MODULUS

The core modulus was calculated by measuring the deflections of a slab of CPR 9005-2 rigid urethane foam.

Dimensions: Length in. 56
Width in. 10
Depth in. 1.75

I_c = Moment of inertia of the beam = 4.47 in.^{4}

LOAD P at midspan lb.	DEFLECTION δ at midspan inch.	P/δ
0.135	0.078	1.73
0.270	0.150	1.80
0.540	0.327	1.66

$P/\delta_{avg} = 1.73$

$$E_c = \frac{P}{\delta} \frac{L}{48 I_c} = 1419$$

We can now evaluate the term

$$(1 - E_c / E_s)$$

From Table I $E_s = 6.6 \times 10^5$

$$(1 - E_c / E_s) = 0.99785$$

APPENDIX C

DEFLECTIONS DUE TO BENDING AND SHEAR

DEFLECTIONS DUE TO BENDING AND SHEAR

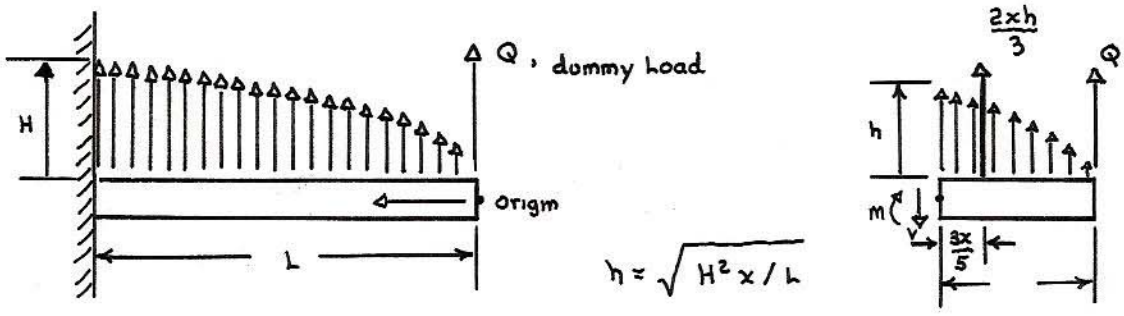

$$M = \frac{3x}{5}\left(\frac{2x\sqrt{H^2x/L}}{3}\right) + Qx \qquad V = \frac{2x\sqrt{H^2x/L}}{3} + Q$$

$$\frac{\partial M}{\partial Q} = x \qquad \frac{\partial V}{\partial Q} = +1$$

$$U = \int_0^L \frac{1}{2}\frac{M^2}{EI}\,dx + \int_0^L \frac{1}{2}\frac{V}{GA}\,dx$$

$$\delta_a = \frac{\partial U}{\partial Q} = \int_0^L \frac{M}{EI}\frac{\partial M}{\partial Q}\,dx + \int_0^L \frac{V}{GA}\frac{\partial V}{\partial Q}\,dx$$

$$\delta_a = \frac{1}{EI}\int_0^L \left[\frac{3x}{5}\left(\frac{2x}{3}\right)\left(\frac{H^2x}{L}\right)^{1/2} + Qx\right][x]\,dx + \frac{1}{GA}\int_0^L \left[\frac{2x}{3}\left(\frac{H^2x}{L}\right)^{1/2} + Q\right][1]\,dx$$

Set $Q = 0$

$$\delta_a = \frac{2H}{5EIL^{1/2}}\int_0^L x^{7/2}\,dx + \frac{2H}{3GAL^{1/2}}\int_0^L x^{3/2}\,dx$$

$$\delta_a = \frac{2H}{5EIL^{1/2}}\,\frac{2}{9}\,x^{9/2}\Big|_0^L + \frac{2H}{3GAL^{1/2}}\,\frac{2}{5}\,x^{5/2}\Big|_0^L$$

$$\delta_a = \frac{4}{45}\frac{HL^4}{EI} + \frac{4}{15}\frac{HL^3}{GA} \qquad \text{Let } I = \frac{bh^3}{12} \quad G = \frac{2}{5}E \quad A = bh$$

$$\delta_a = \frac{48000}{45}\frac{HL}{Eb} + \frac{100}{15}\frac{HL}{Eb} = 1066.7\frac{HL}{Eb} + 6.7\frac{HL}{Eb}$$

$$\%\,\delta \text{ due to Shear} = \frac{6.7}{1066.7+6.7} \times 100 = 0.625\,\%$$

APPENDIX D

MAXIMUM CORE AND SKIN SHEAR STRESSES

SKIN AND CORE SHEAR STRESSES

A core material surrounded by a thin layer of flange material, such that $E_s \quad E_c$, is shown in Figure D1.

FIGURE D1

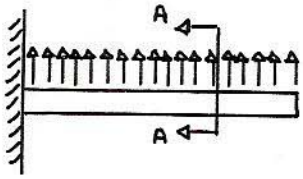

SECTION A-A

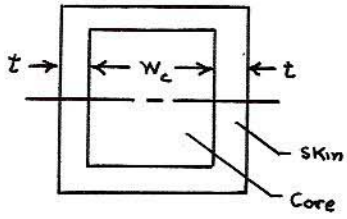

Plain Sections Remain Plain

$$\epsilon_c = \epsilon_s$$

$$\frac{\sigma_s}{E_s} = \frac{\sigma_c}{E_c}$$

$$\frac{E_c}{E_s} = \frac{\sigma_c}{\sigma_s}$$

Equivalent Areas

$$\sigma_c A_c = \sigma_s A_{ce}$$

$$W_{ce} = W_c \, E_c / E_s$$

SECTION A-A
EQUIVALENT AREAS

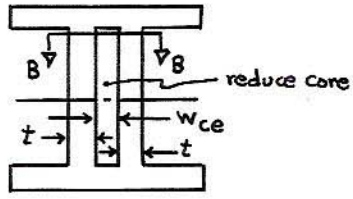

SECTION B-B

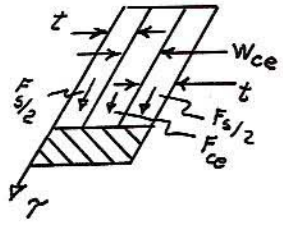

Shear Forces Acting Over Equivalent Areas

$$F_{ce} = \gamma W_{ce} L$$

$$F_s = \gamma \, 2t \, l$$

$$F_{ce} : F_s = \frac{W_c E_c}{2tE_s} \qquad (D1)$$

A ratio between the force in the equivalent core and flange can give an average shear stress ratio when these same forces act over the true core and flange areas, Figure D2.

FIGURE D2

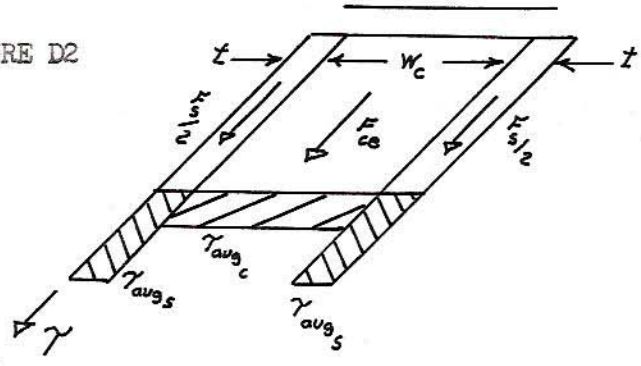

Formula D1 can be used on an airfoil crossection, Figure D3, at midspan to determine a ratio of skin-core shear stresses.

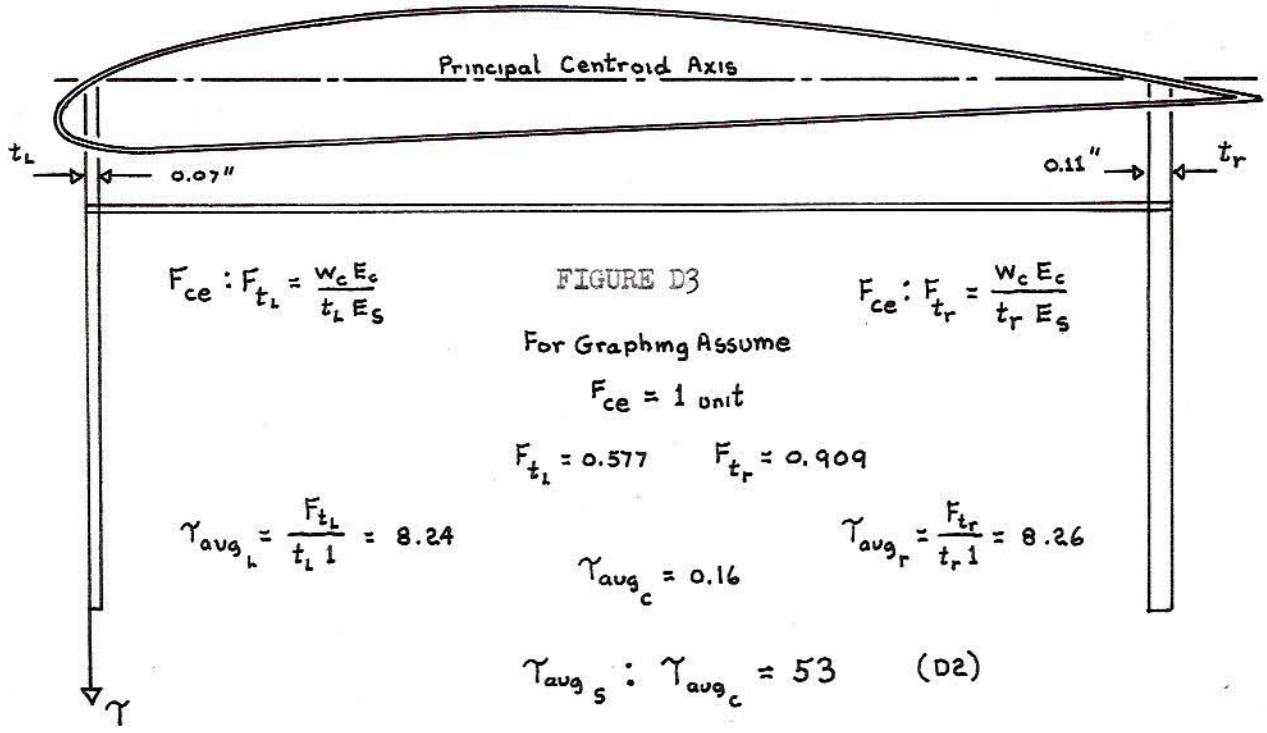

FIGURE D3

Other parallel cuts will all show that the core material resists a substantial portion of the shear load. Therefore the location of the shear center will be influenced by the shear flow distribution in both the core and skin materials.

The maximum allowable composite shear stress can be approximated for an airfoil shown in Figure D3. The airfoil shape is approximated by a rectangular shape so that the math can be used in solving for τ_{max}, Figure D4.

FIGURE D4

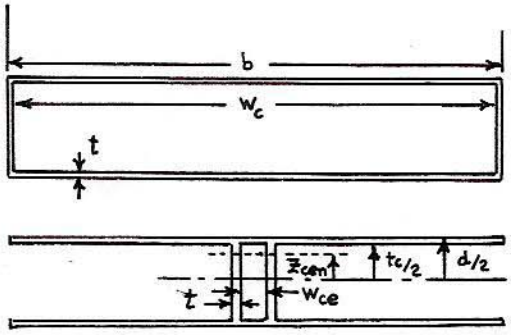

$$\tau_{max} = \frac{V_{max}\, Q@z=0}{I\ width} = \frac{V_{max}\left[(\bar{z}_{cen})(A_{total})\right]}{I\ width}$$

$$I = \frac{b(d^3 - t_c^3)}{12} + \frac{(2t + w_{ce})\, t_c^3}{12}$$

$$width = w_{ce} + 2t \qquad w_{ce} = w_c \, E_c/E_s$$

$$\bar{z}_{cen} = \frac{2(t_c + d)bt + (w_{ce} + 2t)t_c^2}{4t_c(w_{ce} + 2t) + 8bt}$$

$$A_{total} = \frac{t_c}{2}\left(w_{ce} + 2t\right) + bt$$

$$\tau_{max} = \tau_{c_{max}} + \tau_{s_{max}} = \frac{V_{max}\left[\frac{2(t_c + d)bt + t_c^2(2t + w_c E_c/E_s)}{8bt + 4(2t + w_c E_c/E_s)}\right]\left[bt + (2t + w_c \frac{E_c}{E_s})\frac{t_c}{2}\right]}{\left[b(d^3 - t_c^3) + t_c^3(2t + w_c E_c/E_s)\right]\left[2t + w_c E_c/E_s\right]/12} \qquad (D3)$$

Assume : $\tau_{avg_s} = \tau_{s_{max}}$ $\tau_{avg_c} = \tau_{c_{max}}$

And solve (D2) and (D3) simultaneously for a maximum shear load of 10 lb. (7G's). Dimension for a rectangular crossections equivalent to the airfoil in Figure D4 were used.

Dimensions: $t = 0.025, b = 8, w_c = 7.95, t_c = 0.95, d = 1, E_c = 10^3, E_s = 6.6 \times 10^5$

$\tau_{max} = 180\ lb/in^2$

$\tau_{s_{max}} = 177\ lb/in^2$

$\tau_{c_{max}} = 3\ lb/in^2$

Note the skin thickness to resist $\tau_{s_{max}}$ was $t = 0.025 = T_{shear}$

APPENDIX E

MAXIMUM NORMAL SKIN STRESS

MAXIMUM NORMAL SKIN STRESS

The root airfoil shape is approximated as a rectangular crossection so that the moment of inertia in the elastic flexural formula can be written as a function of skin thickness, Figure E1.

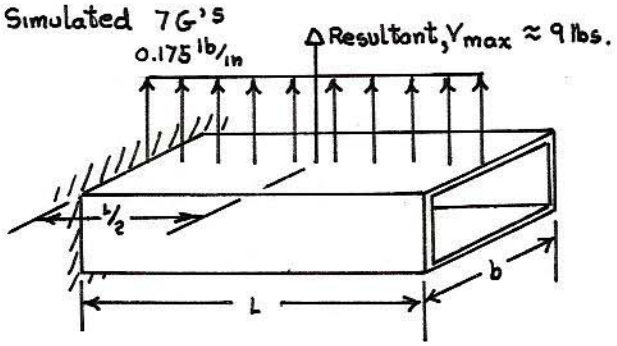

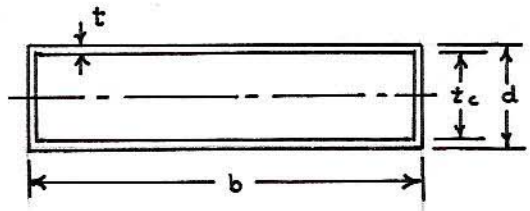

$$I = b/12\,(d^3 - t_c^3) + 2\,\frac{tt_c^3}{12}$$

$$t_c = d - 2t$$

$$I = 1/12\,(\,6t^2tb - 12dt^2b + 8t^3b + 2td^3 - 12d^2t^2 + 12dt^3 - 16t^4\,)$$

b = Root chord = 8 in. L = 50 in.

d = Conservatively low root thickness = 1/4 in.

$$I = 1/12\,(\,12.5t - 51t^2 + 67t^3 - 16t^4\,)$$

From Table I $\sigma_{s_{ult.}} = 6240$ psi $\qquad \sigma = \frac{Mz}{I}$

$$\sigma_{s_{ult.}} = \frac{M_{max}\, z_{max}}{I} = \frac{[9(25)]\ 1/4}{1/12\left\{12.5t - 51t^2 + 67t^3 - 16t^4\right\}} = 6240$$

$$\cancel{16t^4}^{\approx 0} - \cancel{67t^3}^{\approx 0} + 51t^2 - 12.5t + 0.1084 = 0$$

Since t is small

$$t = \frac{+12.5 \pm \sqrt{156 - 22.1}}{102} = 0.0091 \equiv t_{Normal}$$

APPENDIX F

THE STRENGTH ANALYSIS OF

THIN-UNSYMMETRICAL-TAPERED CYLINDERS

THE STRENGTH ANALYSIS OF THINWALLED-UNSYMMETRICAL-TAPERED CYLINDERS

This model assumed that the core was missing and only the skin remained. This restriction was necessary if the original shape of the wing was to be included in a workable mathematical model. Even with this restriction the mathematical model will still give useful information.

The following is a outlined step by step procedure used in evaluating this mathematical model for deflections and stresses.

I) Assume a lift, drag, and torque distribution as a function of span position.

A) Assume a lift distribution L=f(y)
B) Assume a drag distribution D=f(y)
C) Assume a torque distribution T=f(y)

Comments The lift, drag, and torque distributions represent the loads acting on the wing at the aerodynamic center.

II) Calculate direction cosines for aerodynamic center line.

III) Establish a set of reference axis for defining an airfoil shape at any span position.

A) Define the location and shape of the root and tip airfoils using the reference axis.
B) Calculate any other airfoil shape by using analytical geometry.

Comments The airfoils shape was approximated by drawing line segments between 32 points defining the location of the thin skin. The wing shape is defined by drawing straight lines between corresponding points defining the root and tip airfoil shapes.

IV) At any spanwise airfoil section

A) Determine the location of the aerodynamic center
1) Define the location of the root and tip aerodynamic center.
2) Calculate any other aerodynamic center by using analytic geometry.

Comments Any other aerodynamic center location was defined along a

Comments Any other aerodynamic center location was defined along a line drawn between the root and tip aerodynamic center.

B) Determine the centroid location and moments of inertia about a set of centroidal axis referenced parallel with the reference axis.

Comments The accuracy of the centroid location and moments of inertia depend on the skin thickness. The thinner the skin the more accurate the results. ✓

C) Determine the location of the principal centroidal axis and the moments of inertia.

Comments The angle of rotation needed to locate the principal axis is calculated by using the moments of inertia calculated from the previous centroidal axis. This assumed principal axis is then used in calculating the product of inertia. If this product of inertia is not with in a set minimum value then the axis is rotated again until this minimum value is obtained.

SEEMS TO ME AS THOUGH YOU COULD FIND THE PRINCIPAL AXES DIRECTLY, WITHOUT HAVING TO ITERATE.

D) Determine the bending moment, shear force, and torque.
   1) Assume the lift, drag, and torque act at the aerodynamic center.
   2) Use the trapezoidal numerical method for calculating the torque and shear forces.
   3) Use a numerical method analogous to the trapezoidal for calculating the bending moments.
   4) Using the direction cosines previously calculated transfer the loads from the aerodynamic center line to a set of axis parallel to the free stream velocity.
   5) Using the angle of attack and chord angle the loads along the X,Z,Y axis and the XP,ZP,Y axis are calculated.

Comments The program was generalized to handle any shaped load distribution. But interval spacing for elliptic shapes gives the most accurate results.

?

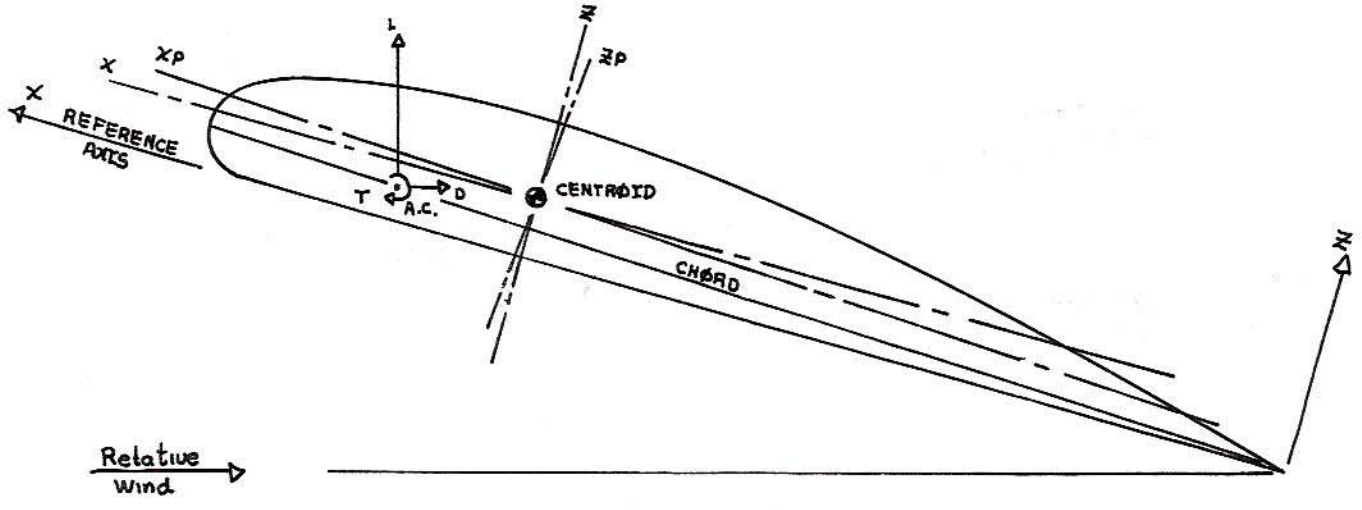

E) Determinethe shear center location and the shear flow due to the shear forces acting along the principal centroidal axis and at the shear center.

Comments The method of closed thin walled sections was used.[5] The accuracy depends on how many points are used to define the shape of the thinwalled crossection and the skin thickness. An error in shear flow values exists because the the formulas assumed nontapered beams and the shear flows were averaged and not curve fitted between points.

F) Determine the constant shear flow due to the torque acting at the shear center.

Comments Again the accuracy depends on a thin wall approximation.

G) Determine the normal skin stresses.

Comments Because the principal centroidal axis and the neutral axis are coincident the normal stress maybe simply calculated from the flexural formula. ONLY BECAUSE LOADS ARE RESOLVED INTO COMPONENTS IN THE PRINCIPAL DIRECTIONS.

H) Determine the twist and deflection

$$\frac{d^2 \text{ Displacement}}{d \text{ Span}^2} = \frac{M}{EI} \qquad \theta = \frac{1}{2(\text{area})^2 G} \Sigma \frac{qs}{t}$$

Comments The differential equation could be solved by using the fourth order runge-kutta numerical method. The flexural rigity (EI) for the skin is equal to the flexural rigidity of the composite. Shear deformations are shown to be small with respect to deformations due to bending, Appendix C.

Unfortunately the runge-kutta and adams-multon methods of solving the differential equations were time consuming. Instead the solutions for deflections for point and distributed loads where used. Starting at the wing root the wing is divided into as many sections as desired for accuracy. Each section is treated as a freebody of constant crossection. The deflections for each section due to moment and shear loads where accumulated using superposition as the program progressed from the root to the tip. Twisting deflections were calculated for each section as a function of the shear flow distribution in the skin due to the torque load. ESSENTIALLY A FINITE ELEMENT PROCEDURE

DIRECTION COSINES FOR AERODYNAMIC CENTER LINE

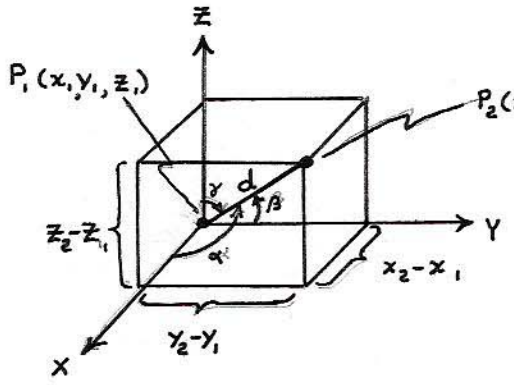

Direction Cosines Defined

$$\lambda = \frac{x_2 - x_1}{d} \qquad \mu = \frac{y_2 - y_1}{d} \qquad \nu = \frac{z_2 - z_1}{d}$$

For two lines

$$\cos\Theta = \lambda_1\lambda_2 + \mu_1\mu_2 + \nu_1\nu_2$$

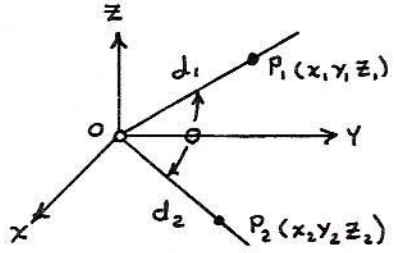

Determination of Direction Cosines For Aerodynamic Center Line

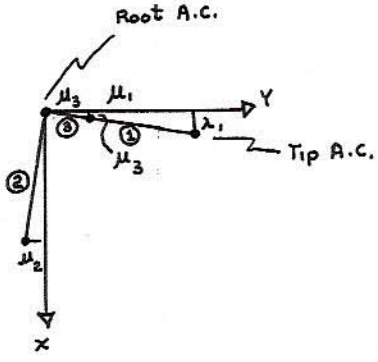

X, Y, Z => Reference axis

λ_1, μ_1, ν_1 calculated From Root and Tip A.C. locations

$$(\mu_1\mu_2 = -\lambda_1\lambda_2) \Rightarrow \frac{\mu_2}{\lambda_2} = -\frac{\lambda_1}{\mu_1}$$

$$(\lambda_2^2 + \mu_2^2 = 1) \Rightarrow \lambda_2 = \sqrt{\frac{1}{(\mu_2/\lambda_2)^2 + 1}}$$

$$\mu_2 = -\frac{\lambda_1}{\mu_1}\lambda_2 \qquad \nu_2 \equiv 0$$

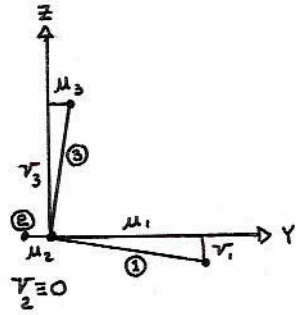

$$(\mu_2\mu_3 = -\lambda_2\lambda_3) \Rightarrow \frac{\lambda_3}{\mu_3} = -\frac{\mu_2}{\lambda_2}$$

$$(\mu_1\mu_3 + \lambda_1\lambda_3 + \nu_1\nu_3 = 0) \Rightarrow \frac{\lambda_3}{\nu_3} = \frac{\nu_1\frac{\lambda_3}{\mu_3}}{\lambda_1\frac{\lambda_3}{\mu_3} + \mu_1}$$

$$\left(\frac{\mu_3}{\nu_3} = -\frac{\nu_1}{\mu_1}\right)$$

$$\left(\mu_3^2 + \lambda_3^2 + \nu_3^2 = 1\right) \qquad \nu_3 = \sqrt{\frac{1}{\left(\frac{\lambda_3}{\nu_3}\right)^2 + \left(\frac{\mu_3}{\nu_3}\right)^2 + 1}}$$

$$\left(\frac{\lambda_3}{\mu_3} = \frac{\lambda_1}{\mu_1}\right) \qquad \mu_3 = -\nu_3\nu_1/\mu_1 \;;\; \lambda_3 = \mu_3\lambda_1/\mu_1$$

AIRFOIL SHAPE DETERMINED AT ANY SPAN LOCATION

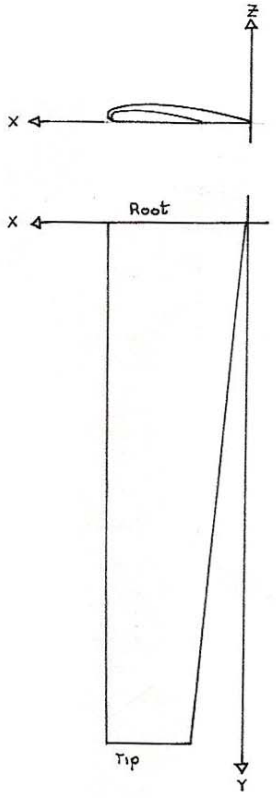

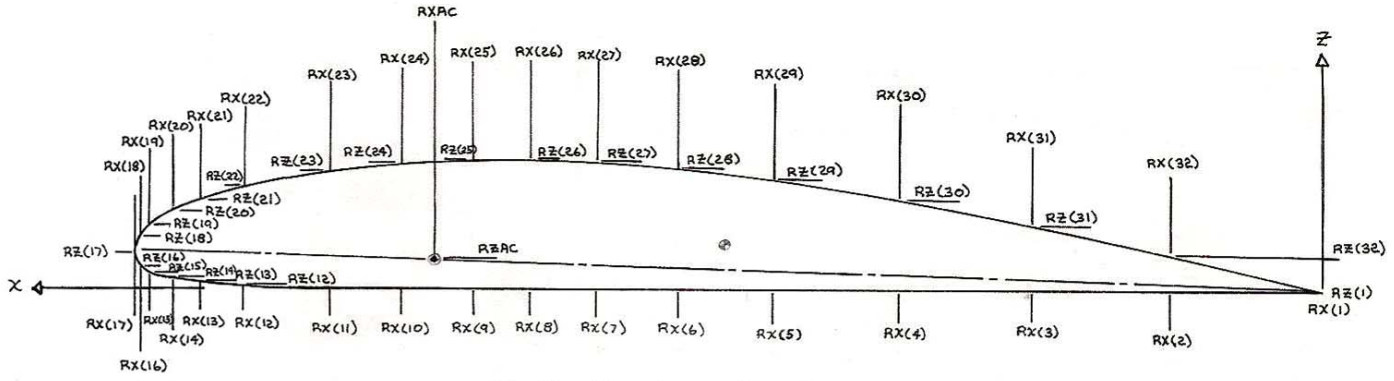

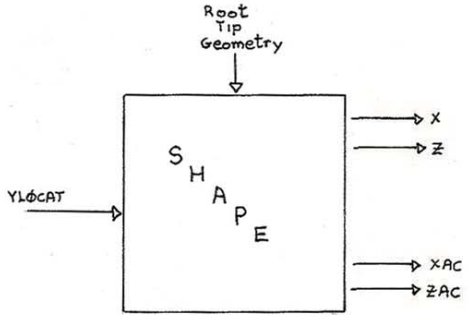

Equation For a Line in three dimensions

$$\frac{x-x_0}{x_1-x_0} = \frac{y-y_0}{y_1-y_0} = \frac{z-z_0}{z_1-z_0}$$

For line 20

$$\frac{X(20)-RX(20)}{TX(20)-RX(20)} = \frac{YLOCAT-YF}{YL-YF} = \frac{Z(20)-RZ(20)}{TZ(20)-RZ(20)}$$

```
      SUBROUTINE  SHAPE (RX,RZ,TX,TZ,RXAC,RZAC,TXAC,TZAC,YF,YL,YLØCAT,X,Z,XAC,ZAC,A,B)
      DIMENSION RX(32),RZ(32),TX(32),TZ(32),X(32),Z(32),A(32),B(32)
      DØ 60 I=1,32
      IF(YLØCAT.EQ.YF) GØ TØ 30
      IF(YLØCAT.EQ.YL) GØ TØ 40
      X(I) = ((TX(I)-RX(I))*(YLØCAT-YF)/(YL-YF)) + RX(I)
      Z(I) = ((TZ(I)-RZ(I))*(YLØCAT-YF)/(YL-YF)) + RZ(I)
      GØ TØ 50
30    X(I) = RX(I)
      Z(I) = RZ(I)
      GØ TØ 50
40    X(I) = TX(I)
      Z(I) = TZ(I)
50    A(I) = X(I)
      B(I) = Z(I)
60    CØNTINUE
      IF(YLØCAT.EQ.YF) GØ TØ 70
      IF(YLØCAT.EQ.YL) GØ TØ 80
      XAC = ((TXAC-RXAC)*(YLØCAT-YF)/(YL-YF)) + RXAC
      ZAC = ((TZAC-RZAC)*(YLØCAT-YF)/(YL-YF)) + RZAC
      GØ TØ 90
70    XAC = RXAC
      ZAC = RZAC
      GØ TØ 90
80    XAC = TXAC
      ZAC = TZAC
90    RETURN
      END
```

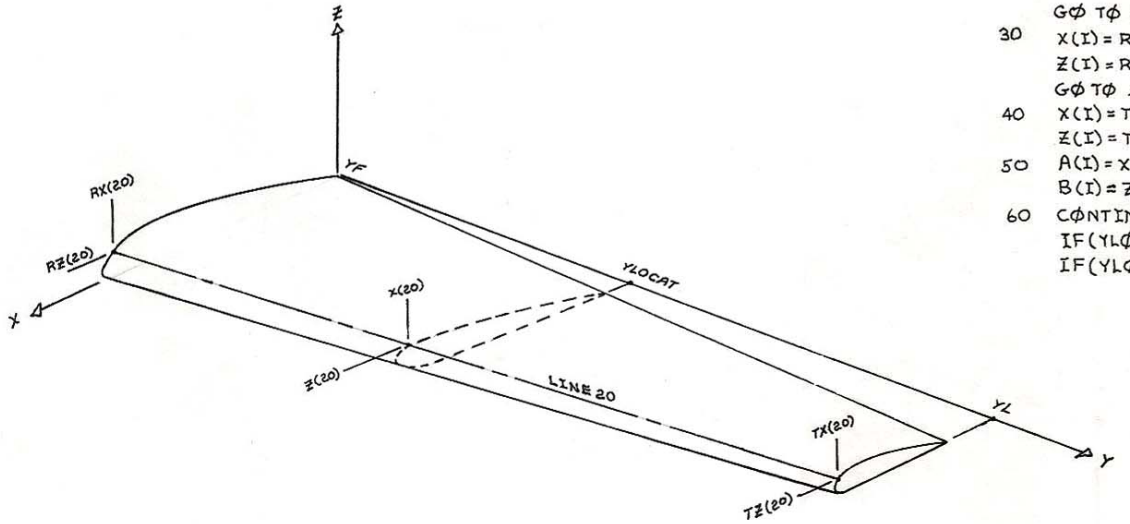

DETERMINE THE LOCATION OF THE PRINCIPAL CENTROIDAL AXIS

and

MOMENTS OF INERTIA

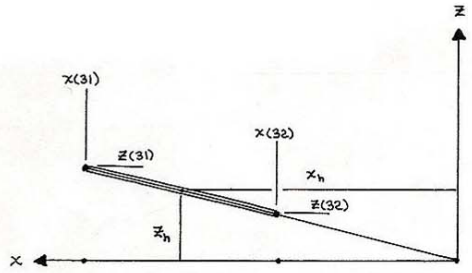

$\Delta z = |z(32) - z(31)| \qquad z_h = \Delta z / 2$

$d = \sqrt{\Delta x^2 + \Delta z^2}$

$\sin\phi = \frac{\Delta z}{d} \qquad \cos\phi = \frac{\Delta x}{d}$

$I_{x_s} = \frac{dt^3}{12} \qquad I_{xz_s} = 0$

$I_{z_s} = \frac{dt^3}{12}$

$A = dt$

$$I_{x_c} = I_{x_s}(\cos\phi)^2 + I_{z_s}(\sin\phi)^2 - 2\cancel{I^0_{xz_s}}\sin\phi\cos\phi$$

$$I_{z_c} = I_{x_s}(\sin\phi)^2 + I_{z_s}(\cos\phi)^2 + 2\cancel{I^0_{xz_s}}\sin\phi\cos\phi$$

$I_x = I_{x_c} + A z_h^2$

$I_z = I_{z_c} + A x_h^2$

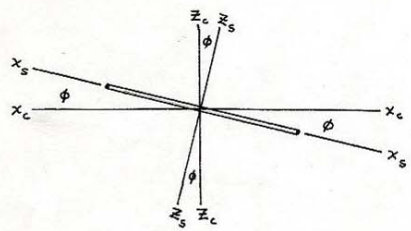

Portion	A	x_h	z_h	Ax	Az	Axz	I_{xc}	I_{z_c}	Ax^2	Az^2	I_x	I_z
1												
2												
⋮												
31												
32												
	ΣA			ΣAx	ΣAz	ΣAxz					ΣI_x	ΣI_z

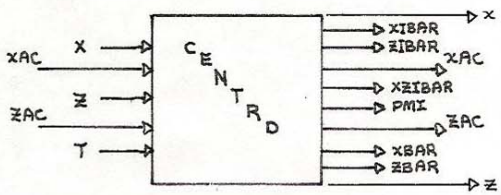


```
      SUBROUTINE CENTRD(X,Z,T,XIBAR,ZIBAR,XZIBAR,XBAR,ZBAR,XAC,ZAC,TANG,PMI)
      DIMENSION X(32),Z(32),XP(32),ZP(32)
      TANG=0.0
      ANG=0.0
    1 AREAT=0
      AXT=0
      AZT=0
      AXZT=0
      XIT=0
      ZIT=0
      DO 10 I=1,32
      J=I+1
      IF(I.EQ.32) J=1
      DELTAX=X(J)-X(I)
      DELTAZ=Z(J)-Z(I)
      DIST=SQRT(DELTAX**2+DELTAZ**2)
      XIS=DIST*(T**3)/12.0
      ZIS=T*(DIST**3)/12.0
      SINANG=DELTAZ/DIST
      COSANG=DELTAX/DIST
      XIC=XIS*(COSANG**2)+ZIS*(SINANG**2)
      ZIC=XIS*(SINANG**2)+ZIS*(COSANG**2)
      AREA=DIST*T
      XBARS=(X(J)+X(I))/2.0
      ZBARS=(Z(J)+Z(I))/2.0
      AX=AREA*XBARS
      AZ=AREA*ZBARS
      AXZ=AREA*XBARS*ZBARS
      AXSQD=AREA*(XBARS**2)
      AZSQD=AREA*(ZBARS**2)
      XI=XIC+AZSQD
      ZI=ZIC+AXSQD
      AREAT=AREA+AREAT
      AXT=AX+AXT
      AZT=AZ+AZT
      AXZT=AXZ+AXZT
      XIT=XI+XIT
      ZIT=ZI+ZIT
   10 CONTINUE
```

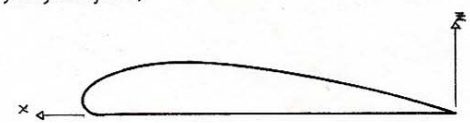


```
      C XBAR=AXT/AREAT
      C ZBAR=AZT/AREAT
      IF(ANG.EQ.0.0) XBAR=CXBAR
      IF(ANG.EQ.0.0) ZBAR=CZBAR
      XIBAR=XIT-AREAT*(CZBAR**2)
      ZIBAR=ZIT-AREAT*(CXBAR**2)
      XZIBAR=AXZT-AREAT*CXBAR*CZBAR
      PMI=XIBAR+ZIBAR
      Y=2.*XZIBAR
      W=ZIBAR-XIBAR
      IF(Y.LT.0.001) RETURN
      ANG=ATAN2(Y,W)/2.
      TANG=TANG+ANG
      DO 20 I=1,32
      XP(I)=X(I)*COS(ANG)+Z(I)*SIN(ANG)
   20 ZP(I)=-X(I)*SIN(ANG)+Z(I)*COS(ANG)
      XACP=XAC*COS(ANG)+ZAC*SIN(ANG)
      ZACP=-XAC*SIN(ANG)+ZAC*COS(ANG)
      DO 30 I=1,32
      X(I)=XP(I)
   30 Z(I)=ZP(I)
      XAC=XACP
      ZAC=ZACP
      GO TO 1
      END
```

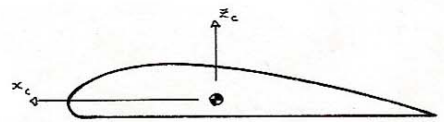

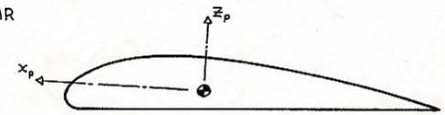

NUMERICAL DETERMINATION OF THE BENDING MOMENT, SHEAR FORCE, AND TORQUE

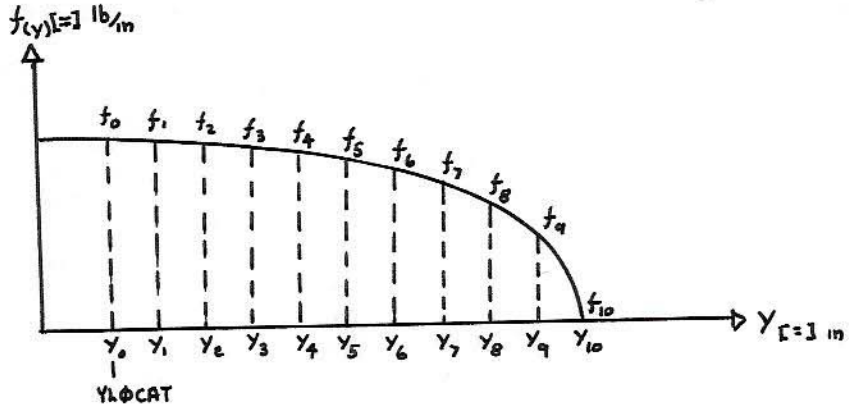

$$\text{Force} = \int_a^b f_{(y)}\,dy = \sum_{i=0}^{n} \frac{H}{2}(f_i + f_{i+1}) = \frac{H}{2}\left[f_0 + 2f_1 + 2f_2 + \cdots + 2f_{n-1} + f_n\right] \quad [=] \text{ lb}$$

$$\text{Moment} = \int_a^b f_{(y)}\,y\,dy = \sum_{i=0}^{n} \frac{f_i + f_{i+1}}{2} H \frac{y_i + y_{i+1}}{2} \quad [=] \text{ lb.in.}$$

$$= \frac{H}{4}\Big[f_0 y_0 + f_0 y_1 + f_1 y_0 + 2 f_1 y_1 + f_1 y_2 + f_2 y_1 + 2 f_2 y_2 + f_2 y_3 + f_3 y_2 + \cdots$$

$$\cdots + 2 f_{n-1} y_{n-1} + f_{n-1} y_n + f_n y_{n-1} + f_n y_n \Big]$$

SHEAR FLOW IN CLOSED THIN-WALLED SECTIONS

The following is quoted from Bruhn [5]. In this solution, we determine the centroid of the internal shear flow system for bending of the closed section about axis X without twist. This point is called the shear center. The external shear load can the be resolved into a shear force acting through the shear center plus a torsional moment about the shear center.

We start the solution, as shown in the example problem, by assuming the shear flow is zero at the cut section. This section will bend without twist if the external shear load acts through the shear of the open section.

The closed section will be assumed to bend without twist, and the resulting shear flow pattern will be determined.

The equation for angular twist per inch length of the beam is,

$$\Theta = \frac{1}{2AG} \Sigma \frac{qs}{t}$$, where s equals the length of a web or wall.

or $$2A\Theta = \frac{1}{G} \Sigma \frac{qs}{t}$$. The right hand side of this equation represents the total shearing strain around the cell which must be zero for no twist of cell. Since G is constant, we can assume it as unity as only relative values of strain are needed in the solution. Thus the total shearing strain δ around cell is proportional to,

$$\delta = \Sigma \frac{qs}{t}$$

If the cell is not to twist the relative twist of δ must be cancelled by adding a constant shear flow around the cell to give a total shearing strain. This shearing strain for a constant shear flow is,

$$\delta = q \sum \frac{s}{t}$$

If this constant shear flow is added to the shear flow for the open section then the shear flow for the closed section results.

Now that the shear flow pattern for the closed section is known the shear center can be located by summing moments about some point and dividing by the shear force.

$$\bar{x} = \frac{\Sigma M_o}{\Sigma F_z}$$

The moment of the external load will cause a torque about the shear center. The resulting shear flow is calculated by

$$q = \frac{T}{2A}$$

COMPUTER PROGRAM LISTING

INPUT DATA FORMAT

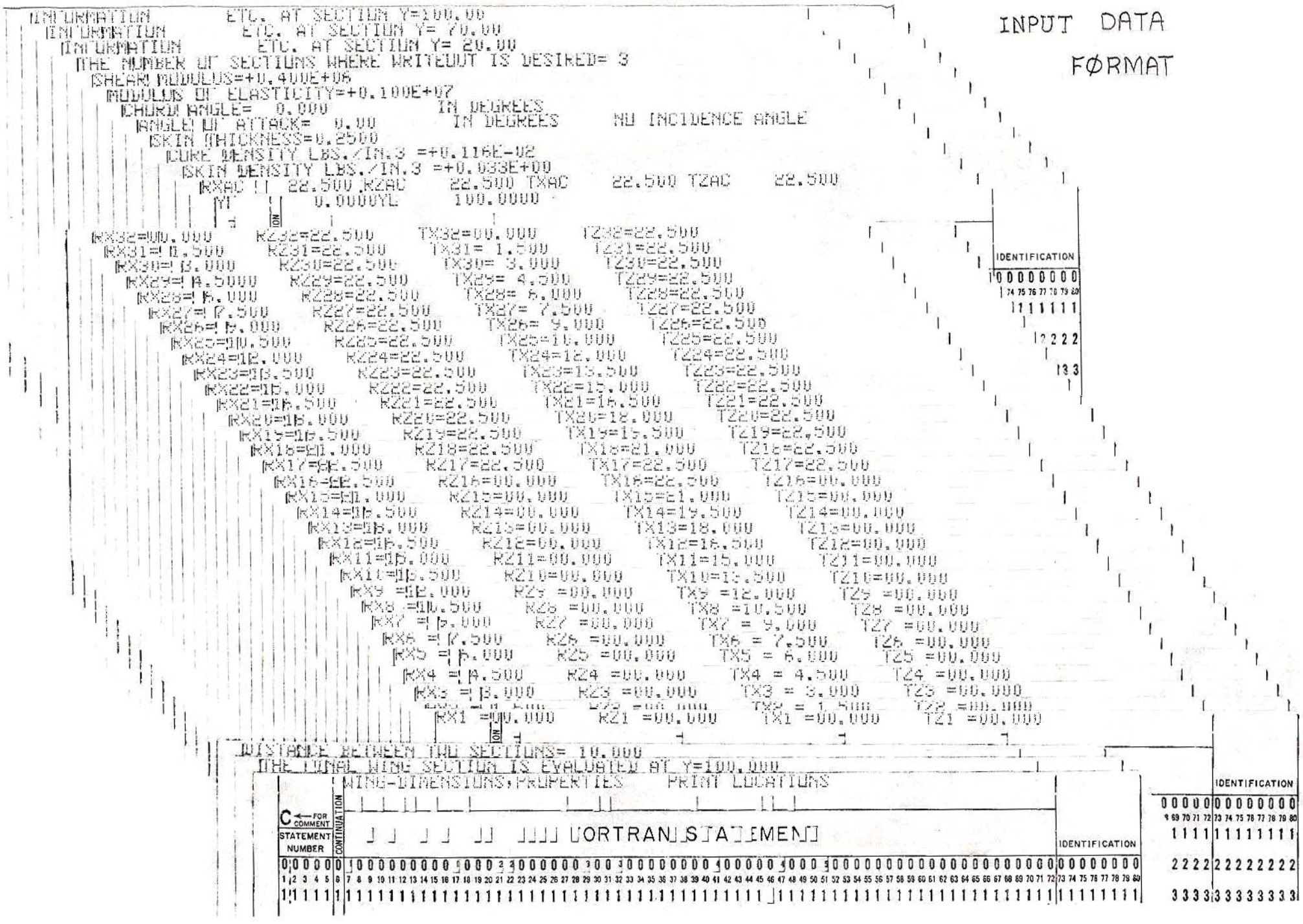

EXAMPLE PROBLEM

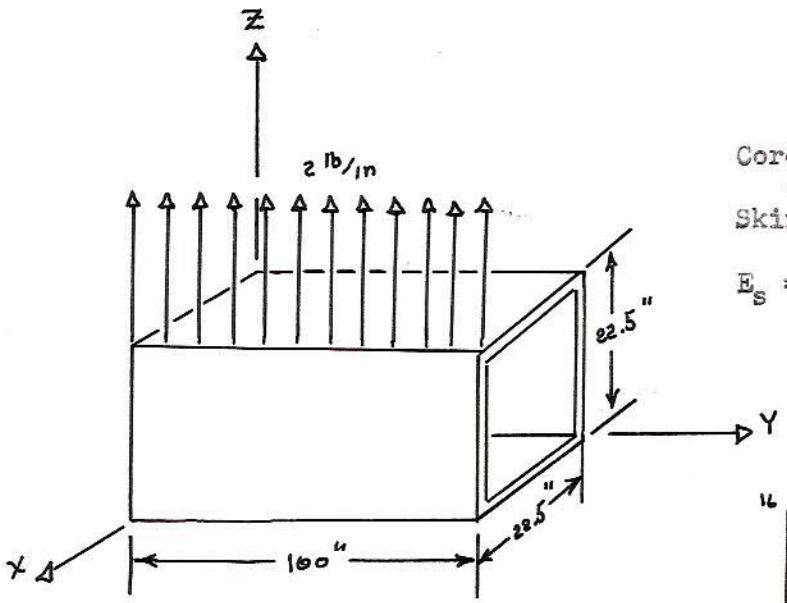

Core density = 0.00116 lb/in

Skin density = 0.033 lb/in

$E_s = 6.6 \times 10^5$

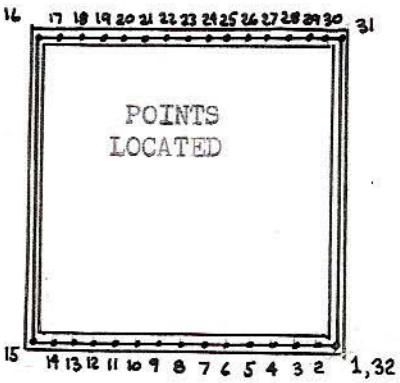

RESULTS

TIP DEFLECTION

Analytic	0.0132 in	Error	0.7%
Numeric	0.0131 in		

MIDSPAN CALCULATIONS

Moment of inertia about X and Z axis

Analytic	1895.2 in^4	Error	0.2%
Numeric	1898.5 in^4		

Product of inertia

Analytic	0	No difference
Numeric	0	

Shear in the X and Z direction

Analytic	100 lb	No difference
Numeric	100 lb	

Moment about the X and Z axis

Analytic	2500 in lb
Numeric	2500 in lb

Centroid location

	X	Z	
Analytic	11.25	11.25	No difference
Numeric	11.25	11.25	

Shear center location

	X	Z	
Analytic	11.25 in	11.25 in	Error 0.2%
Numeric	11.279 in	11.251 in	

Shear flow distribution

Analytic	See page D12	No noticable difference
Numeric	See computer output listing	

Normal stress distribution at point 16

Analytic	29.70 psi	Error 0.2%
Numeric	29.63 psi	

Weights

Core

Analytic	58.725 lb	No difference
Numeric	58.725 lb	

Skin

Analytic	74.25 lb	No difference
Numeric	74.25 lb	

SHEAR FLOW DISTRIBUTION

Equations Used

$$q = -\frac{V_z}{I_x} \Sigma \bar{z} A \quad , \quad \Sigma qs/t \quad , \quad q \Sigma s/t$$

Open Section $\quad I_x = 1898.5 \quad V_z = +100 \quad \frac{V_z}{I_x} = 0.0526731630$

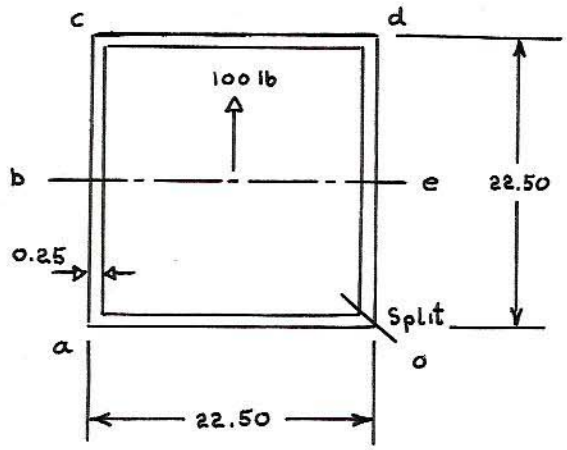

$q_o = 0$

$q_a = q_o - \frac{V_z}{I_x}(-0.25)\,22.5\,(0.25)$

$q_a = +3.333223598$

$q_b = q_a - \frac{V_z}{I_x}(-5.625)\,11.25\,(0.25)$

$q_b = +4.166529497$

$q_c = q_b - \frac{V_z}{I_x}(5.625)\,11.25\,(0.25)$

$q_c = +3.33323598$

$q_d = q_c + \frac{V_z}{I_x}(11.25)\,22.5\,(0.25)$

$q_d = 0$

$q_e = q_d - \frac{V_z}{I_x}(5.625)\,11.25\,(0.25)$

$q_e = -0.8333058990$

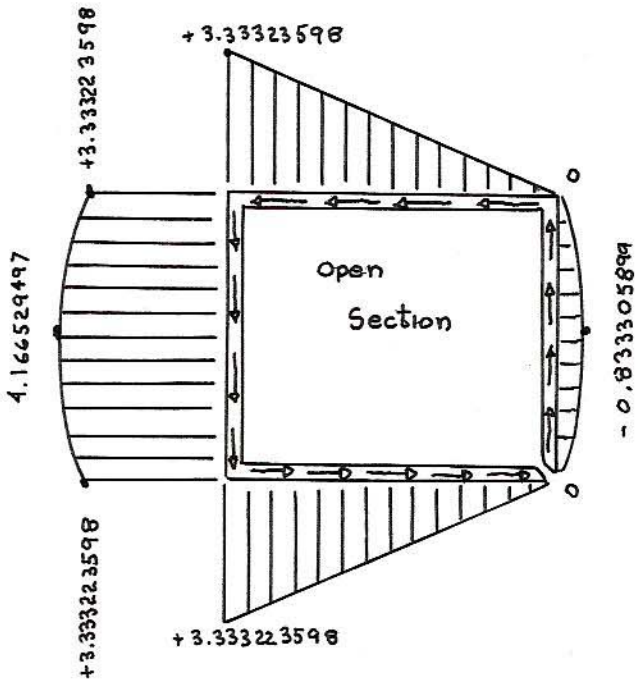

Calculating Unbalance Closed Section

$$\Sigma \frac{\bar{q}_b}{t} = 2\left[\frac{q_a}{2}\frac{22.5}{0.25} + \frac{q_a 11.25}{0.25} + \frac{(q_b - q_a)\,0.667\,(11.25)}{0.25} + \frac{q_e\,0.667\,(11.25)}{0.25}\right]$$

$$\Sigma \frac{\bar{q}_s}{t} = 599.9802476$$

Constant Shear Flow to resist Unbalance

$$q \Sigma \frac{s}{t} = -599.9802476$$

$$q = -1.666611799$$

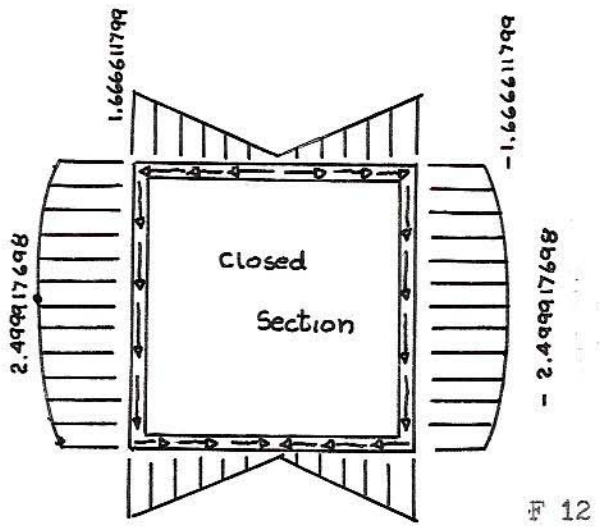

COMPUTER OUTPUT LISTING

FOR THE

EXAMPLE PROBLEM

APPENDIX G

THIN WALLED CANTILEVER

BOX BEAM

DEFLECTIONS

THIN WALLED CANTILEVER BOX BEAM DEFLECTIONS

Using the same 7G uniform lift distribution and the same moment of inertia assumed in Appendix E an approximation of the maximum wing tip deflections can be made by the formula;

$$y_{max} = \frac{w L^4}{8EI}$$

$$y_{max} = \frac{0.175\ (51)^4}{8\ (6.6 \times 10^5)\ 1/12 \left\{12.5t - 51t^2 + 67t^3 - 16t^4\right\}}$$

$$y_{max} = \frac{2.69}{12.5t - 51t^2 + 67t^3 - 16t^4}$$

$t = 0.01$ m. $\quad y_{max} = 24$ in.

$t = 0.025$ in $\quad y_{max} = 10$ in.